buildings

MDPI

Article

Numerical Analysis of Shallow Foundations with Varying Loading and Soil Conditions

Muhammad Rehan Hakro [1,*], Aneel Kumar [1], Mujahid Ali [2,3,*], Agha Faisal Habib [1], Afonso R. G. de Azevedo [4], Roman Fediuk [5,6,*], Mohanad Muayad Sabri Sabri [6], Abdelatif Salmi [7] and Youssef Ahmed Awad [8]

[1] Department of Civil Engineering, Mehran University of Engineering & Technology, Jamshoro 76020, Pakistan; aneel.kumar@faculty.muet.edu.pk (A.K.); dr.faisal@faculty.muet.edu.pk (A.F.H.)
[2] Department of Civil and Environmental Engineering, Universiti Teknologi Petronas, Seri Iskandar 32610, Malaysia
[3] Department of Civil Engineering, Faculty of Engineering, Universiti Malaya, Kuala Lumpur 50603, Malaysia
[4] LECIV—Civil Engineering Laboratory, UENF—State University of the Northern Rio de Janeiro, Av. Alberto Lamego, 2000, Campos dos Goytacazes, Rio de Janeiro 28013-602, Brazil; afonso@uenf.br
[5] Polytechnic Institute, Far Eastern Federal University, 690922 Vladivostok, Russia
[6] Peter the Great St. Petersburg Polytechnic University, 195251 St. Petersburg, Russia; mohanad.m.sabri@gmail.com
[7] Department of Civil Engineering, College of Engineering, Prince Sattam Bin Abdulaziz University, AlKharj 16273, Saudi Arabia; a.salmi@psau.edu.sa
[8] Structural Engineering, Faculty of Engineering and Technology, Future University in Egypt, New Cairo 11835, Egypt; youssef.ahmed@fue.edu.eg
* Correspondence: rehan.hakro@faculty.muet.edu.pk (M.R.H.); mujahid_19001704@utp.edu.my (M.A.); roman44@yandex.ru (R.F.)

Citation: Hakro, M.R.; Kumar, A.; Ali, M.; Habib, A.F.; de Azevedo, A.R.G.; Fediuk, R.; Sabri, M.M.S.; Salmi, A.; Awad, Y.A. Numerical Analysis of Shallow Foundations with Varying Loading and Soil Conditions. *Buildings* **2022**, *12*, 693. https://doi.org/10.3390/buildings12050693

Received: 26 April 2022
Accepted: 19 May 2022
Published: 23 May 2022

Abstract: The load–deformation relationship under the footing is essential for foundation design. Shallow foundations are subjected to changes in hydrological conditions such as rainfall and drought, affecting their saturation level and conditions. The actual load–settlement response for design and reconstructions is determined experimentally, numerically, or utilizing both approaches. Ssettlement computation is performed through large-scale physical modeling or extensive laboratory testing. It is expensive, labor intensive, and time consuming. This study is carried out to determine the effect of different saturation degrees and loading conditions on settlement shallow foundations using numerical modeling in Plaxis 2D, Bentley Systems, Exton, Pennsylvania, US. Plastic was used for dry soil calculation, while fully coupled flow deformation was used for partially saturated soil. Pore pressure and deformation changes were computed in fully coupled deformation. The Mohr–Columb model was used in the simulation, and model parameters were calculated from experimental results. The study results show that the degree of saturation is more critical to soil settlement than loading conditions. When a 200 KPa load was applied at the center of the footing, settlement was recored as 28.81 mm, which was less than 42.96 mm in the case of the full-depth shale layer; therefore, settlement was reduced by 30% in the underlying limestone rock layer. Regarding settlement under various degrees of saturation (DOS), settlment is increased by an increased degree of saturation, which increases pore pressure and decreases the shear strength of the soil. Settlement was observed as 0.69 mm at 0% saturation, 1.93 mm at 40% saturation, 2.21 mm at 50% saturation, 2.77 mm at 70% saturation, and 2.84 mm at 90% saturation of soil.

Keywords: soil; shallow foundation; degree of saturation; loading; FEM; Plaxis 2D; settlement

1. Introduction

Foundations are typically built to achieve standards of strength and serviceability to support structure and equipment. Under serviceability conditions, the foundation must perform so that the structure or equipment it supports may fulfil its design purpose under typical operating loads. Settlement or other motion limits are commonly used to explain these serviceability limitations. Strength requirements are to ensure that the foundation has enough reserve strength to withstand enormous loads that may occur due to extreme environmental conditions or other sources. Serviceability or settlement and strength criteria can be addressed as separate design jobs in most circumstances. Serviceability is a long-term issue for the foundation that might be influenced by time-dependent consolidation characteristics. Foundation strength, also known as bearing capacity, may be a short-term issue, such as the construction of an embankment on an undrained clay foundation, or a long-term one in which the maximum foundation load may arise at an undetermined period in the future [1]. In designing shallow foundations, settlement is one of the main parameters [2,3]. Settlement assessment of shallow foundations and carrying capacity calculation are significant and typical geotechnical problems [4], and have been widely investigated as deterministic problems. The most prominent scientific publications emphasize the importance of the interaction between soil and footing settlement and portray this as of the impact on footing shape [5–14]. According to Das et al. [15], factoring in settlement is more important than considering the bearing capacity in shallow foundation design, particularly for foundation widths greater than 1.5 m, which is more common in engineering practices.

There are two kinds of shallow foundation settlements—immediate and secondary settlements of compression. Immediate settlement is encountered as load application after the structure is constructed [16,17]. Settlement of footings depends on many variables, including the shape and size of the footing, embedding depth, layering, soil mass non-homogeneity, type of loading conditions, and saturation degree [18].

Loads are transferred to near-surface unsaturated soils, which change with hydrological events at shallow footings. Recent advances in unsaturated soil mechanics demonstrate that matric suction has a large influence on the strength and settlement of soils. Shallow footings have been located and built on near-surface unsaturated soils, ignoring the influence of matric suction on soil shear strength [2,19–24].

At present, it is possible to analyze foundations by finite element methods, and limit equilibrium [25–28] and the finite difference method [29] have been widely used in recent years to determine the bearing capacity and settlement of footings.

The hydrological process in heterogeneous porous media has received a lot of interest and study [30–33], using analytical or numerical methods [34,35], since layered soil is significantly more widespread than homogeneous soil. The numerical modeling of shallow foundations in unsaturated layered soil using variably saturated conditions under varying loading and stiffness of soil has hardly been reported.

In recent years, the geotechnical problem of shallow foundation response was investigated by its stochastic nature. Scientific publications have investigated the uncertainty quantification of the material uncertainty in cohesive and non-cohesive soil materials. Uncertainty quantification analyses have led to probability density functions regarding many aspects of soil response such as the non-linear response of sand or the porous consolidation and failure of clays. Finally, footing settlement response under spatial variability of soil has also been investigated [11,36–44]. Sivakugan and Johnson [45] developed a probabilistic system based on settlement records in the literature to calculate the risk associated with settlement prediction methods. Settlement and bearing capacity of foundation models with various vertical cross-sectional shapes under the vertically applied load action are presented on non-cohesive subsoil bases. Models of foundations of rectangular, wedge, and T vertical cross-sectional forms were experimentally tested and verified, with a study generally showing foundations with higher bearing capacity and lower settlement with rectangular vertical cross-sectional shapes rather than with wedge and T shapes, from which lower bearing capacity and higher settlement were reported [46].

The mechanical behavior of unsaturated soils, depending on the form of the soil and various pore-water and pore-air conditions, can be interpreted using either modified total stress or a modified efficient stress system. The technique proposed is tested in unsaturated cohesive soils with model base test results [22].

Due to challenges in measuring strength and deformation parameters as functions of matric suction and/or degree of saturation, only a few studies have been conducted to examine the effect of rainfall infiltration on the stability of shallow footings (DoS) [47–56]. The spatial and temporal change in the degree of saturation (DoS) of soil is impacted directly by numerous hydrological parameters, including water table depth, infiltration, flood, and drought [57,58].

Changes in moisture content and groundwater level highly affect the strength and the deformation properties of soil, thereby on the whole overlaying construction. However, geotechnical engineers neglect this topic in most cases, assuming that soil conditions will always remain unchanged. Thus, it is considered one of the foremost causes of foundation settlement, leading to various adverse effects on the overlaying constructions. It appears necessary to use various ground modification methods to stabilize the soil, and strengthen and restore foundations [59–62].

Floods, excessive rainfall, seasonal changes, and drought substantially impact foundation settlement behavior, which may exceed limits [63–77]. For locations where the near-surface soil is partially saturated during the structure's design life, the present design approach can be either conservative or unconservative, depending on the type of hydrological event. This process can cause settlements to exceed acceptable limits, jeopardizing the structure's stability. As a result, it is vital to estimate the additional settlements that may occur due to changes in water conditions to offer an adequate margin of safety [78,79].

The current study is dedicated to observing footing settlement under various degrees of saturation and matric suction in Plaxis 2D FEM Software, Bentley Systems, Exton, Pennsylvania, US. The numerical modeling of Plaxis 2D is to be conducted on soil from the Jamshoro area to assess settlement of shallow foundations under different soil saturation and loading conditions. This research consists of three phases: compilation of all the in situ and laboratory data available and extraction of soil profiles for each plot in the area; the use of well-known correlation to determine model parameters; and numerical modeling.

2. Materials and Methods

2.1. Experimental Methods

Undisturbed soil samples, namely shale and weathered limestone, were obtained by rotatory drilling. After sample collection, samples were transported to the laboratory of Mehran University Jamshoro for testing. Several tests were performed on the soil samples including sieve analysis and calculation of liquid limit, plastic limit, shear strength, and unconfined compression strength.

Extensive soil investigation and laboratory work have been conducted in the Jamshoro study area. The collected soil sample profile has a characteristic two-layer soil structure followed by a stiff layer of rocks, as shown in Figure 1. The soil was classified as A-7-5 according to AASHTO (8th edition), while CH was based on the USCS classification system. After soil extraction, the Casagrande testing method was used to calculate the Atterberg limits. The liquid limit was determined as 70%, the plastic limit as 30%, the shrinkage limit as 15%, and the specific gravity of the shale as 2.60. The modified proctor test found a maximum dry density of 1.9 g/cm^3. Equations (1) and (2) were used to calculate the undrained cohesion (Cu) and the modulus of elasticity (E), which are represented in Table 1. The angle of internal friction and cohesion was determined using the shear box test as 11° and 22 (kN/m^2).

The modulus of elasticity is determined using the following relationship:

$$E = 180\ Cu \tag{1}$$

$$Cu = qu/2 \tag{2}$$

where Cu is the undrained cohesion, and qu is the ultimate load applied.

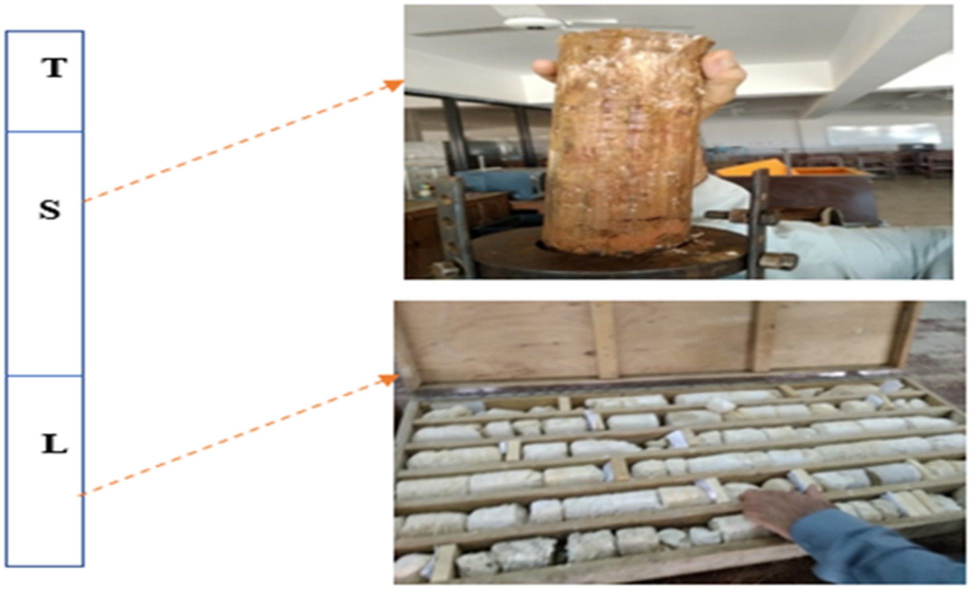

Figure 1. Typical soil profile of study area.

Table 1. Soil properties.

Parameters	Values
Angle of internal friction ϕ (degrees)	11°
Cohesion (kN/m^2)	22
E (kN/m^2)	24,711
Poisson's ratio v;	0.3
Dilatancy angle (Ψ)	0

The modulus of the welasticity of soil was determined with the correlation mentioned above and cited from the work of Sivrikaya et al. [80,81]. Thus, E is determined as 24,711 kN/m^2, as mentioned in Table 1.

The Poisson's ratio was calculated as suggested by Pusadkar et al. [82] for CH and CL soil, determined as 0 from the relationship (Ψ = ϕ − 30).

2.2. Numerical and Boundary Conditions

The finite element analysis was conducted using Plaxis 2D ultimate v.21, Bentley Systems, Exton, PA, USA. The plain strain condition using the elastoplastic Mohr–Columb model was selected to simulate the behavior of the soil sample (Jamshoro Shale), with the parameters selected as drained. The overlaying foundation is modeled as a typical linear elastic with non-porous media. The symmetry axis and the proper vertical boundaries are constrained laterally. In both vertical and horizontal directions, the bottom boundary was restrained. Under load, soil and rock exhibit highly non-linear behaviour. The well-known Mohr–Coulomb model can be thought of as a first-order approximation of real soil behaviour. Mohr–Coulomb model parameters such as the modulus of the elasticity of soil, shear strength parameters such as cohesion, and angle of internal friction are inserted as input parameters. The dilatancy angle was zero. As a first-order (linear) simulation of actual soil efficiency, the known Mohr–Coulomb constitutive law was used. Hook's law of isotropic elasticity underpins the linear elastic portion of the MCM. Based on the Mohr–Coulomb failure criterion, the component is perfectly plastic. The MCM does not incorporate either the stress nor the stress-path dependencies of the stiffness. In general, failure stress states can be adequately represented using the Mohr–Coulomb failure criterion and effective strength parameters. There was no assumption of material hardening or softening. Because there was no subterranean water in the profile at testing, no pore pressure was assumed during the study [83].

The distributed load was applied on the footing as a line load in Plaxis; and through the staged construction option, the footing was initially activated after the line load. After the geometry of the model was established and the material properties were assigned to all clusters, the next step was to divide the geometry into elements in mesh generation. A medium-sized mesh was selected for more accuracy and reduced program processing time. The Plaxis 2D software allows the 'Robust Triangulation Scheme' to automatically generate finite element meshes. A relatively coarse mesh may fail to capture the domain's significant responses, whereas probability accumulates numerical errors beyond the optimally fine mesh. Additionally, very fine meshing should be avoided because calculations take excessive time. With further provision of local refinements, as required by the merit of the problem and the position of the answer points in the numerical simulation, any simple meshing scheme can be adopted.

The plane strain model and 15 nodes were selected to simulate the soil medium. Plane strain models are used for shapes with a (more or less) uniform cross-section, stress state, and loading scheme along a certain length perpendicular to the cross-section (z direction). It is assumed that there are no displacements or strains in the z direction. Plane strain assumes that the problem being analyzed has an infinite length normal to the segment of the plane being analyzed. In a plane strain analysis, the out-of-plane displacement (strain) is zero by definition. The axisymmetric analysis is commonly applied to circular tunnels. For circular structures with a (more or less) uniform radial cross-section and loading scheme around the central axis, an axisymmetric model is utilized, in which the deformation and stress state are assumed to be the same in any radial direction. Compared to the 6 noded triangular components, it offers more nodes, and Gauss points to assist in the comparatively precise determination of displacements and stresses. The model dimensions have been selected so that the deformation in the soil does not intersect the model's boundaries. The width of the soil model was set as 20 m and the depth as 10 m. There is a need to determine the initial stresses in Plaxis simulations. For the specification of these stresses, two possibilities are available in the software: 'K_0 procedure' and 'gravity loading'. As a guideline, in the case of a horizontal surface and for any soil layer and phreatic lines parallel to the surface, the 'K_0 procedure' should be used. The "standard fixity" condition was employed in the numerical model. On the vertical edges, horizontal fixity was added, while the model's bottom edge is considered to be non-yielding and constrained from both vertical and horizontal movements. The numerical modeling was performed using an official Plaxis 2D v.21 Ultimate Licence at Saint Petersburg polytechnic university, Russian Federation, subscription type: CNTI—SPbPU (1006650066). Figure 2 shows the geometry of the model, in which the foundation modeled with a plate element and positive and negative interfaces was applied. The positive and negative interfaces are applied to soil and foundation.

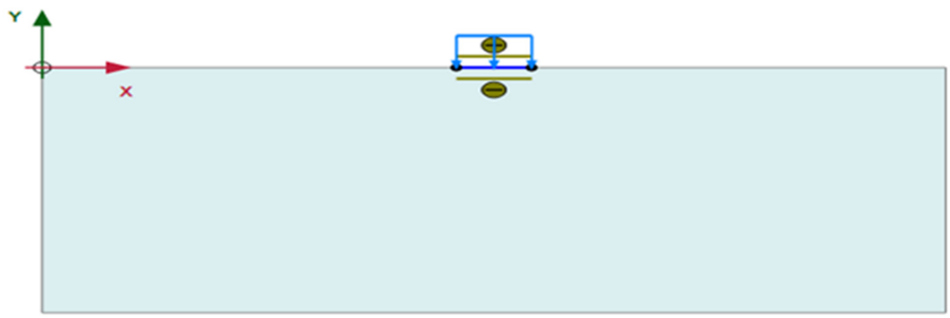

Figure 2. Model geometry.

3. Results and Discussion

Foundation settlement under load model conditions was simulated similar to under field conditions using Plaxis 2D. The initial stress state of the soil was generated before construction. The initial stage is often called the K_0 procedure. K_0 and R_{inter} are 0.67 and 1.0, respecively. The displacements after this initial stage are set to zero. The model's geometry from the second phase is inherited, and the vertical load is applied. The footing has a uniform load of 12 or 24 KPa, roughly corresponding to the equivalent load of a typical one-story and two-story building [84]. Settlement of the footing under a load of 12, 24, and 36 KPa is depicted in Figure 3, and it is noted that with the increase in load, settlement increased. The corresponding bending moment of the footing is shown in Figure 4.

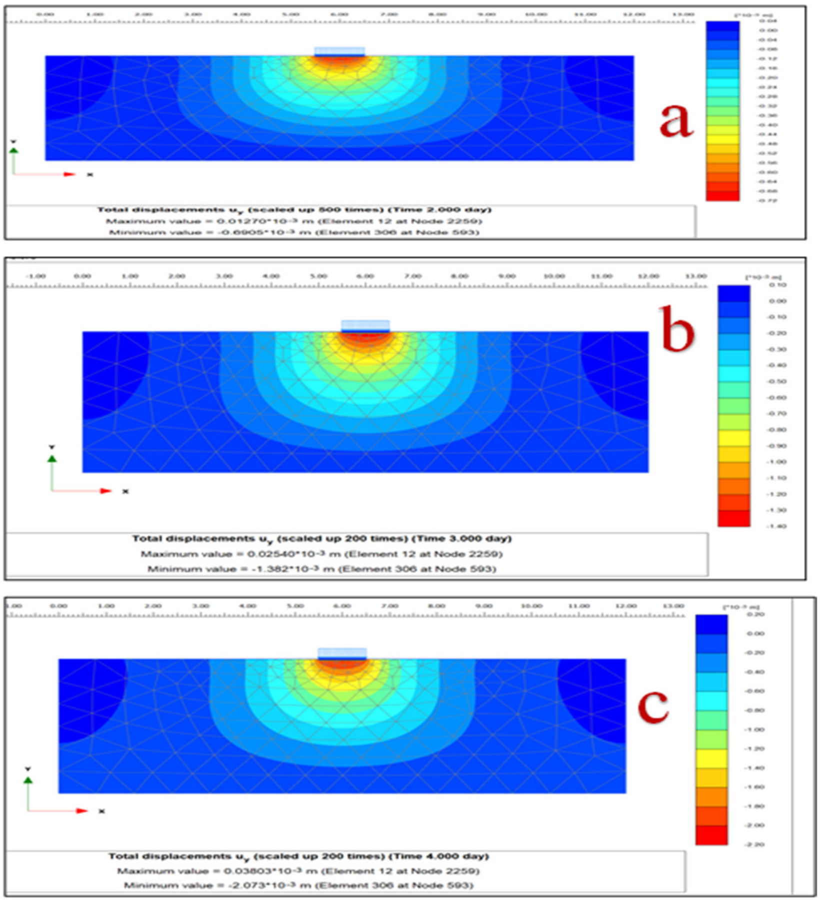

Figure 3. Settlement of the footing under a load of (**a**) 12, (**b**) 24, and (**c**) 36 KPa.

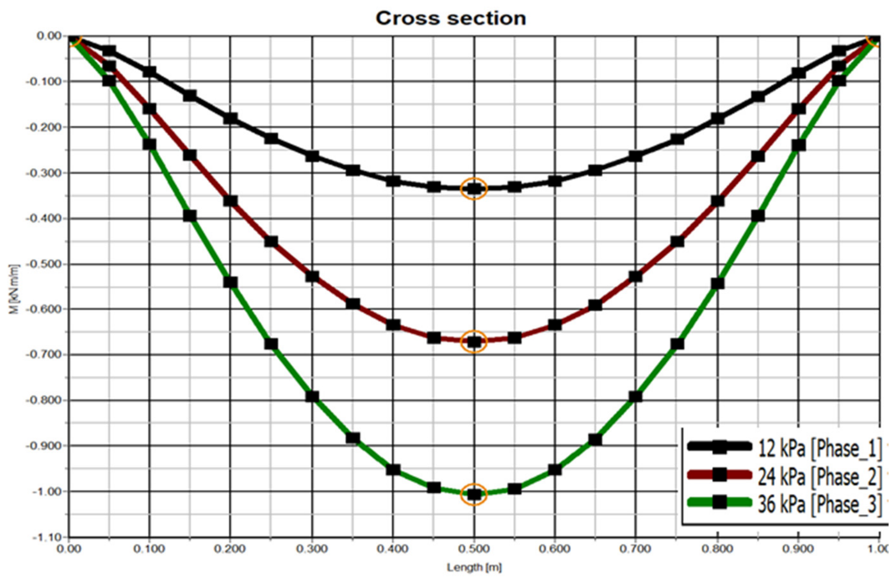

Figure 4. Bending moment of the footing.

With the intensity of load increased to 200 KPa, the load–deformation curve under a load of 50, 100, and 200 KPa is shown in Figure 5, and the crorresponding observed settlements are 3.7, 9.8, and 42.2 mm, respectively. Numerical modeling was performed by Altaweel et al. [85]. The purpose was to offer a numerical study that uses 3D Plaxis application's finite element analysis to evaluate the impact of clay soils on foundation settlement. This effect is explored using a 1 m wide strip foundation under different situations.

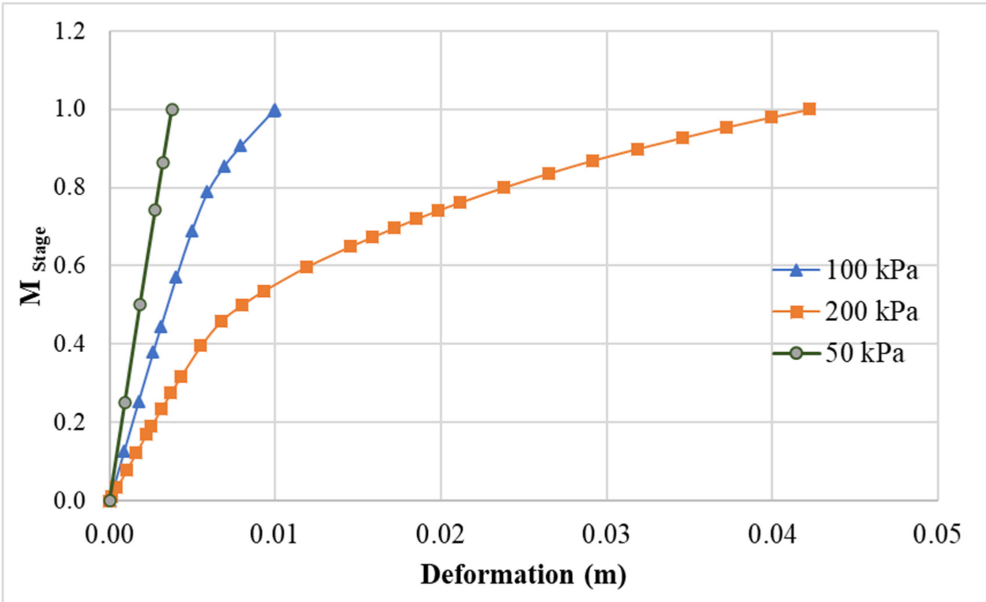

Figure 5. Load–deformation curve.

In Figure 6, numerical modeling was performed on two-layered soil, with a difference in stiffness. Settlement decreased with the inclusion of a higher stiffness layer. In turn, the bending moment of the footing decreased, as shown in Figure 7. The thickness of the shale layer (top layer) was 1 m and that of the lower layer was 9 m. Similarly, settlement decreased considerably in the limestone layer (rock layer) below the shale layer. The effect of the deformation modulus on the deformation properties is shown in Figure 8. The thickness of the footing was 0.75 m. The inteface between the shale and limestone layers influenced the deformation properties, as shown in Figure 9.

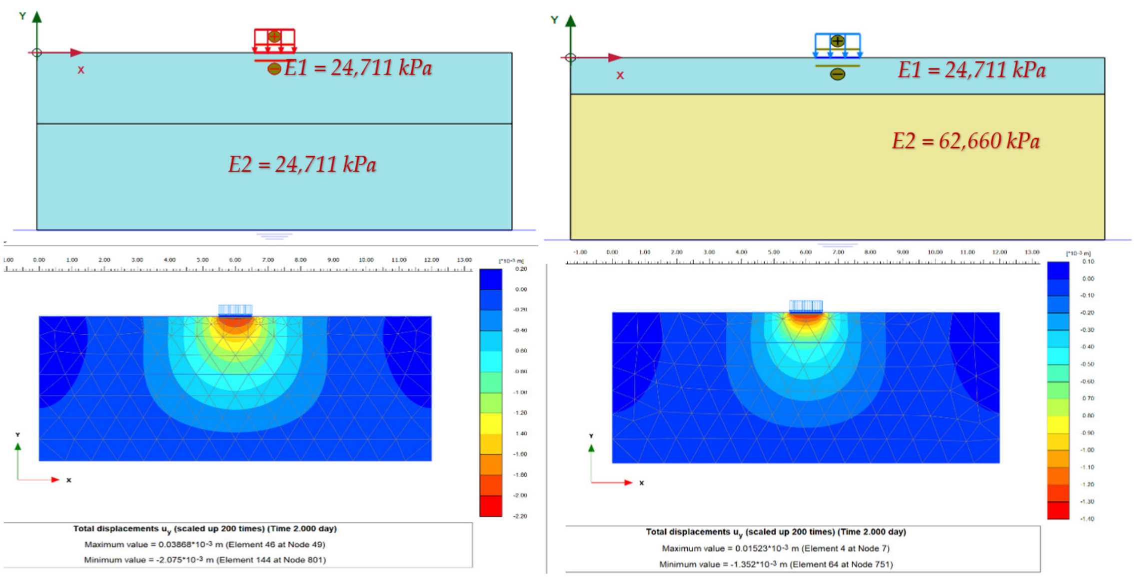

Figure 6. Effect of the stiffness of the layer.

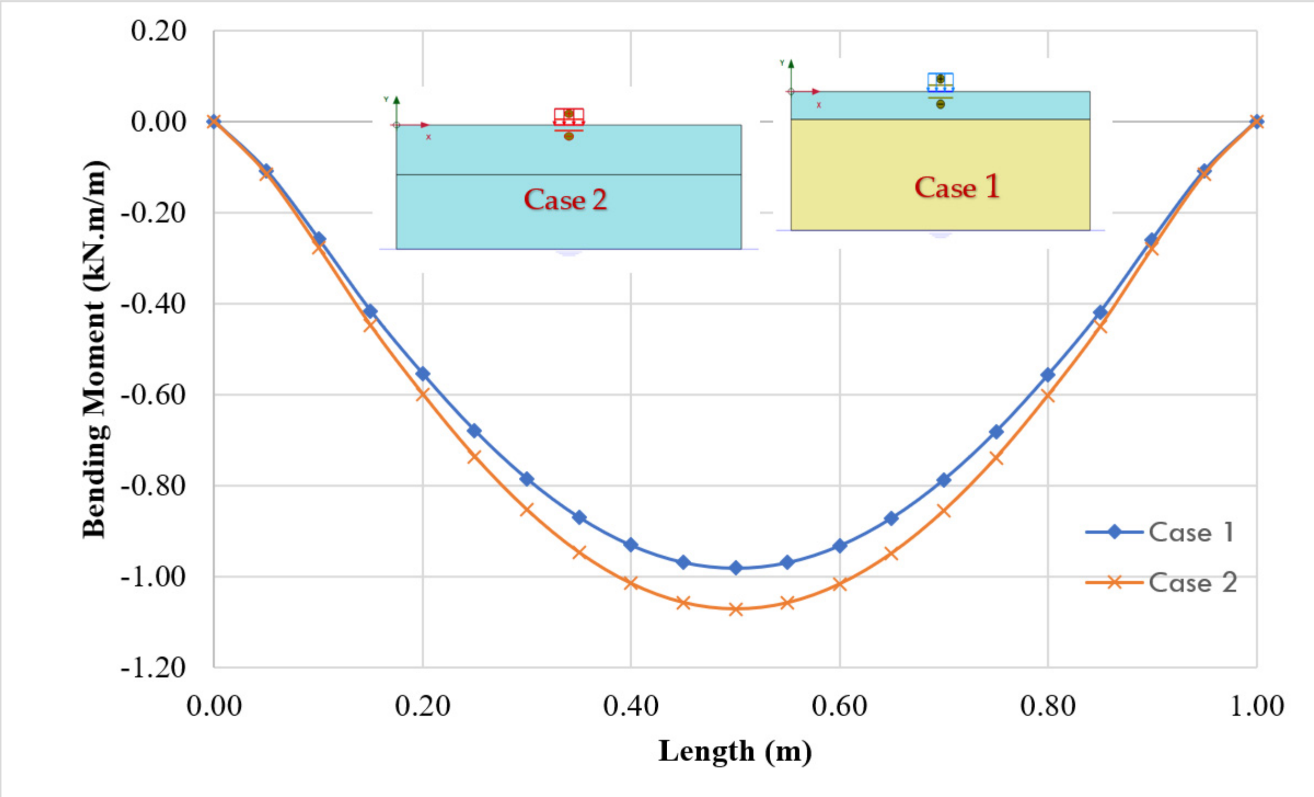

Figure 7. Effect of the stiffness of the layer on the bending moment.

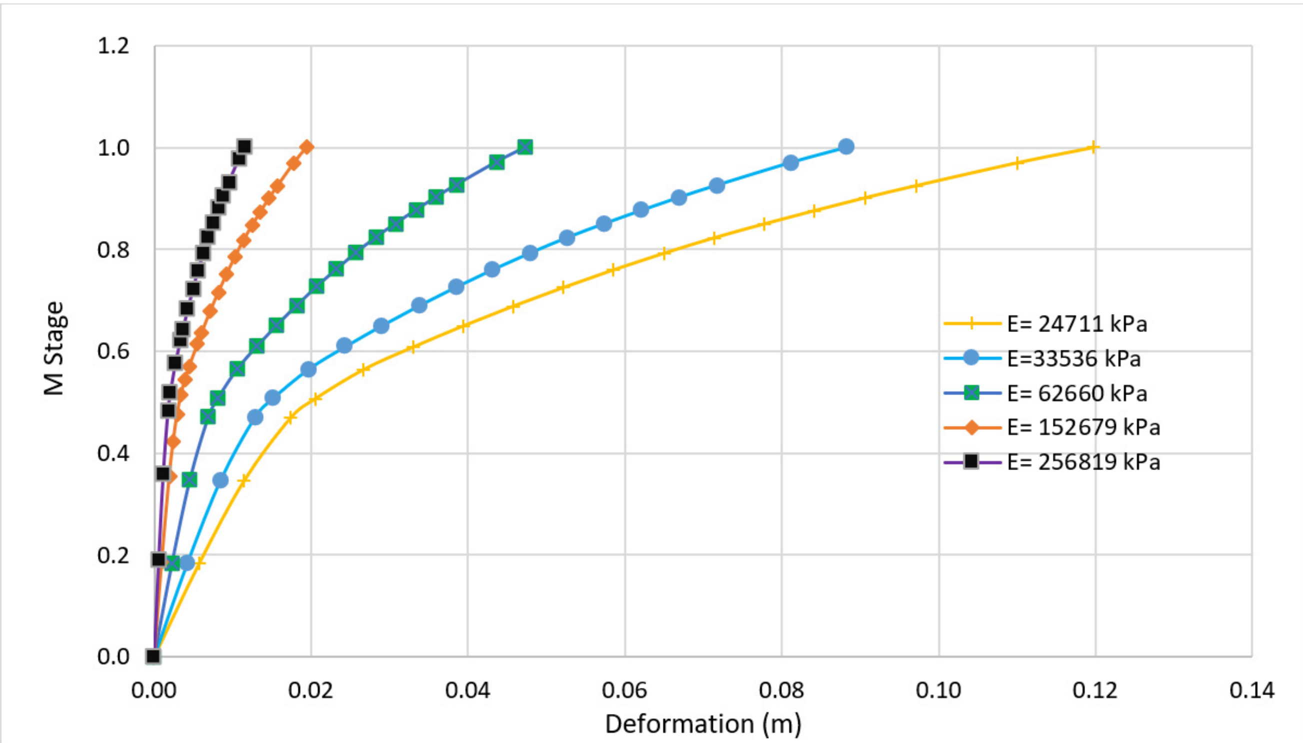

Figure 8. Effect of the modulus of elasticity on the deformation properties.

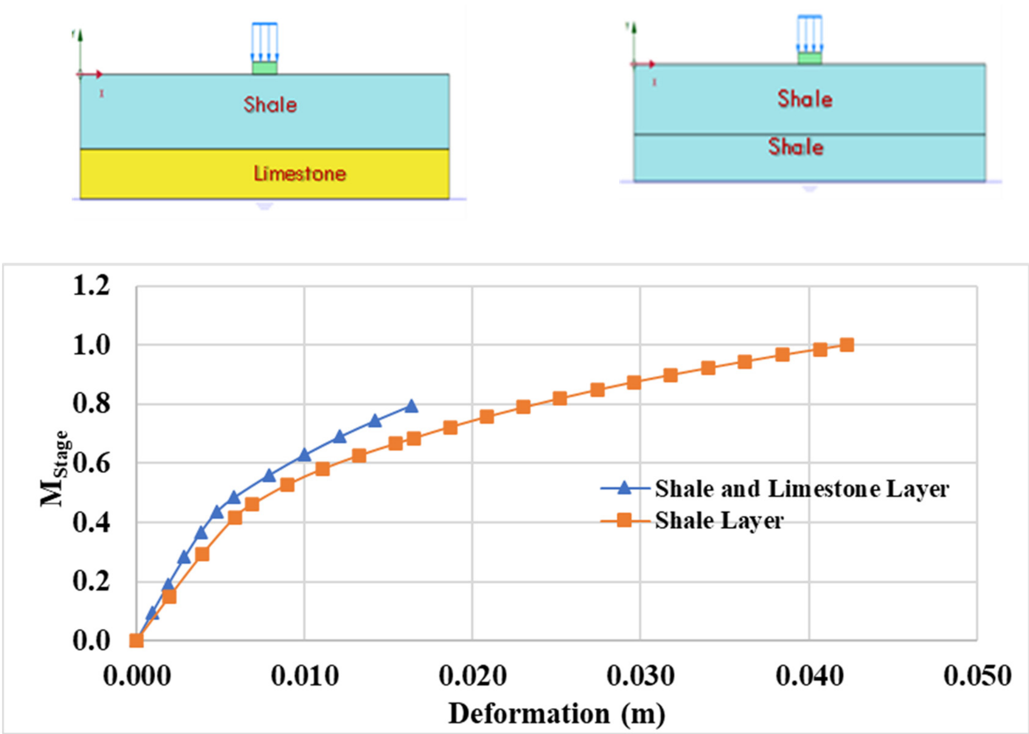

Figure 9. Interface between the shale and limestone layers.

In Figure 10, settlement decreased due to unsaturated conditions. This is due to matric suction dominating settlement. The unsaturated conditions were modeled with fully coupled flow deformation. The research presented by Liu et al. [86] is a novel investigation into the numerical modelling of rainfall-induced shallow landslides in unsaturated layered soil using the variably saturated flow equation. A one-dimensional, transient, unsaturated groundwater flow problem in two-layered soil was investigated. The permeability coefficient of the layers was different. This demonstrates that the lowest FOS occurs during a rainstorm event at the interface between two consecutive soil layers.

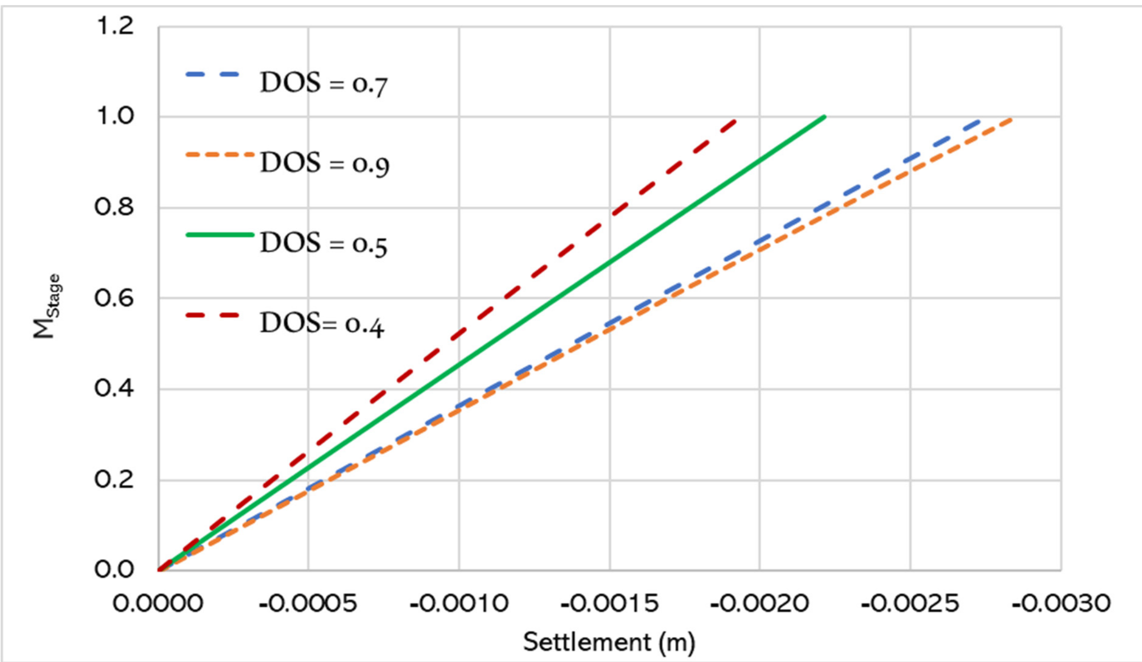

Figure 10. Effect of dry and unsaturated conditions.

In Figure 11, the effect of the degree of saturation on settlement of footing is depicted; the degree of saturation varied from 0.4 to 0.9, and as the degree of saturation increased, settlement increased. Changing the matric suction and saturation level affects the soil shear modulus, which directly impacts shallow foundation elastic settling. In general, raising the matric suction (or lowering the saturation level) significantly impacts foundation settlement reduction [87]. The change in the degree of numerical saturation modeling was performed in FORTON with the cam clay model by Mehnedritta and Sawant [88] to observe the effect of saturation on settlement. In that study, the degree of saturation varied from 85% to 95% and 100%, and they stated that the instantaneous displacement is reported to be significantly lower at 100 percent saturation than at lower degrees of saturation. At 100 percent saturation, the load is transmitted to the soil particles and water present in the voids, resulting in a decrease in soil volume due to pore water expulsion alone. However, in a partially saturated situation, the volume can be reduced by compressing the air voids and the water and soil particles.

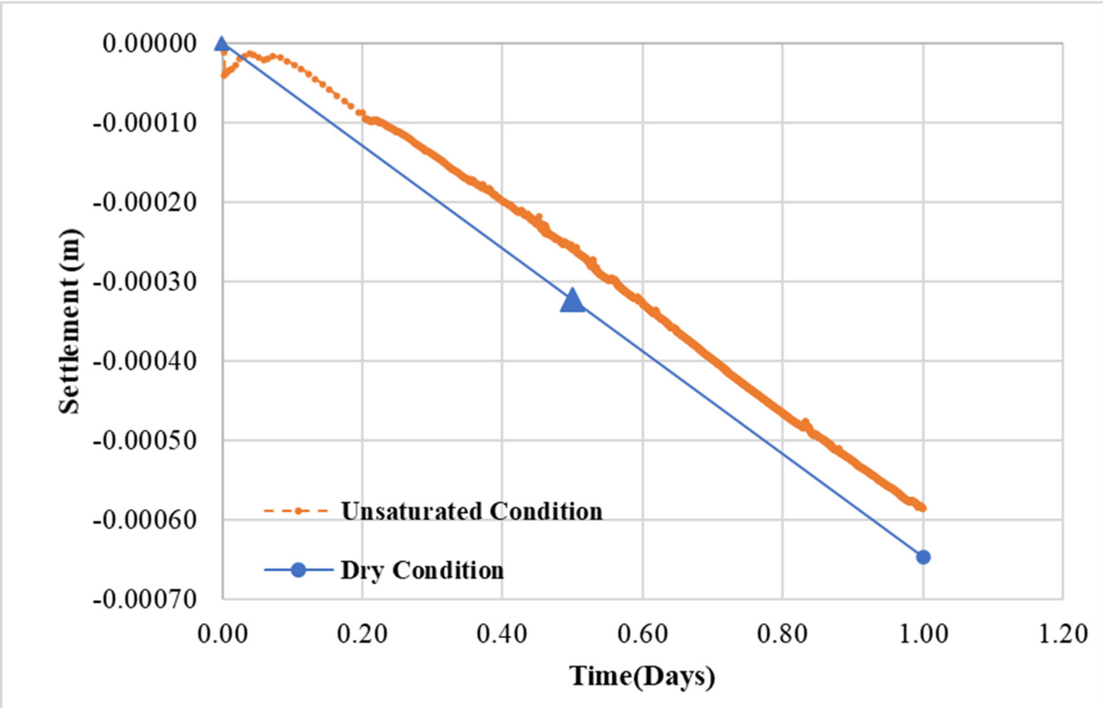

Figure 11. Effect of the degree of saturation (DOS).

Figure 12 shows the variation in deformation with time from settlement to heave of the footing due to the development of matric suction in the soil under a load of 12 KPa. Figure 13 shows the contours of settlement and heave. In the first phase of dry conditions and the second phase, arbitrary small rainfall is applied to soil to activate negative pore pressure (matric suction). In dry conditions, under the load, settlement is depicted in Figure 13 as 0.00080 m; and in unsaturated conditions, under the same load, the footing shows a heave of 0.000485 m. The generation of negative pore pressure is the main reason behind this phenomenon. The soil water characteristic curve parameters were taken from the database of Plaxis 2D for clay type of soil. The soil water characteristic curve governs the behavior of matric suction of soil, more often termed as SWCC, which is the relationship between negative pore pressure and degree of saturation. The matric suction depends on the soil type and permeability. For simplicity, the same modulus of elasticity for unsaturated soil is assumed as saturated soil.

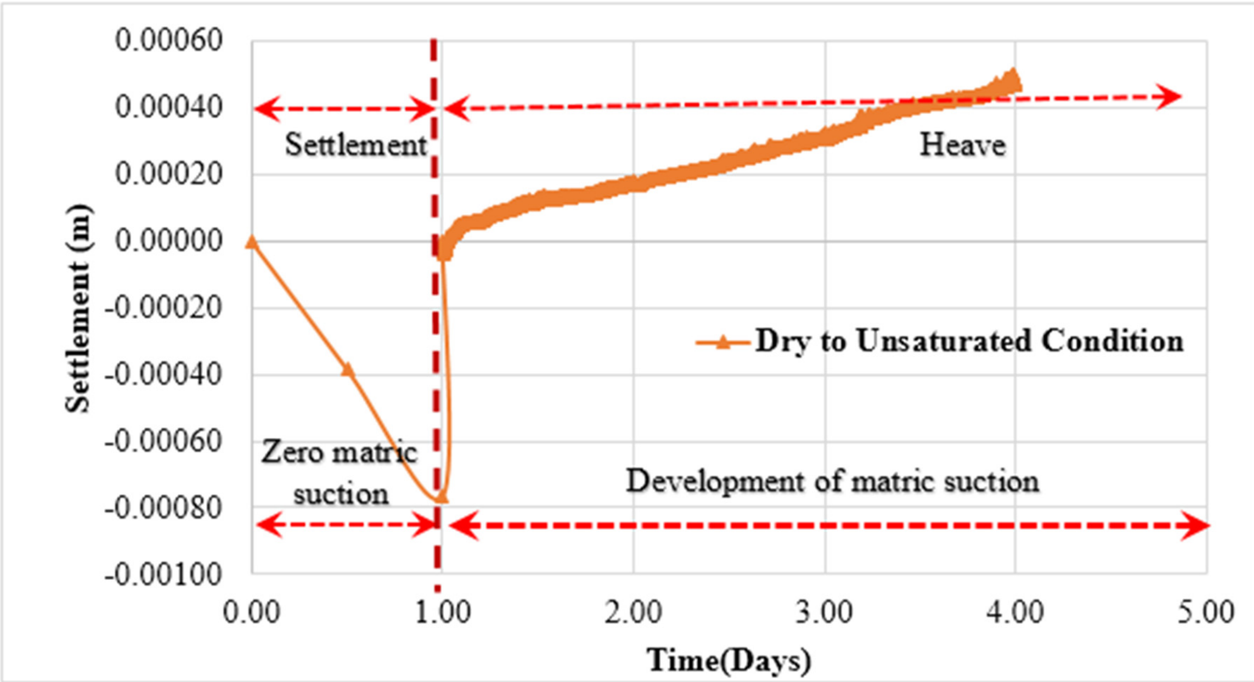

Figure 12. Change of soil water conditions.

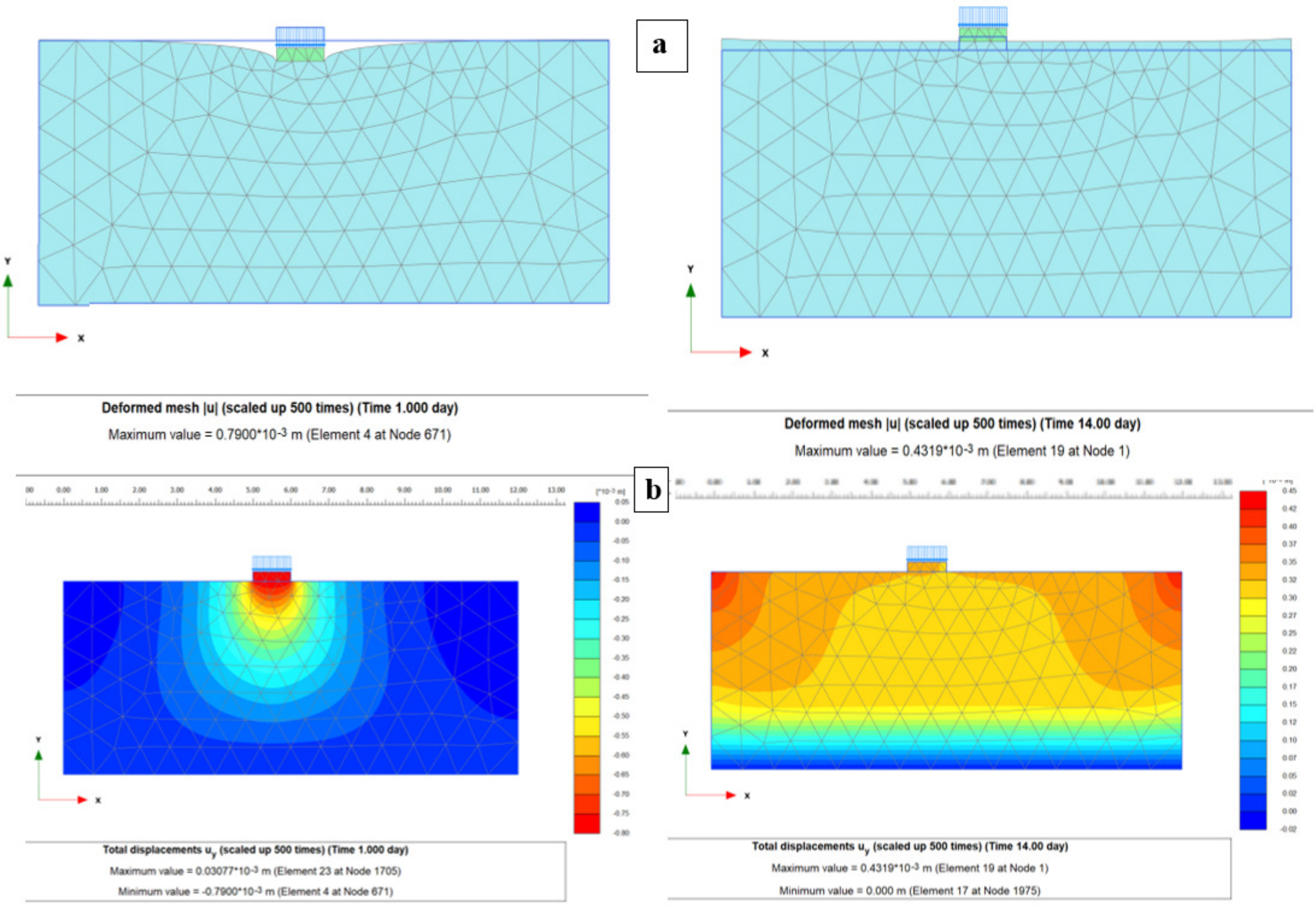

Figure 13. Effect of soil water conditions: (**a**) deformed mesh (**b**) contour.

4. Conclusions

Finite element research was undertaken using the PLAXIS 2D to predict the settlement behavior of shallow foundations. Analyses were carried out utilizing the Mohr–Columb model under different soil conditions, loading, and saturation degree (saturated and unsaturated). Based on the findings of this study, the following conclusions can be drawn:

- Settlement is depicted with load–settlement and time-dependent settlement variation. Settlement decreased with increased soil stiffness (the modulus of elasticity) and increased with loading intensity.
- Settlement at the center of footing at a load of 200 KPa is 28.81 mm, which is less than 42.96 mm in the case of the full-depth shale layer. Thus, settlement reduced by 33 percent when the underlying limestone rock layer was present. These results show that the presence of an underlying limestone layer decreasse settlement of the shallow foundation to significant level.
- The footing settlement under various degrees of saturation (DOS) was observed. It was found that settlment is increasing by increasing the degree of saturation, which increases pore pressure and decreases the shear strength of the soil. Settlement was observed as 0.69 mm at 0% saturation 1.93 mm at 40% saturation, 2.21 mm at 50% saturation, 2.77 mm at 70% saturation, and 2.84 mm at 90% saturation of soil. The increase in the degree of the saturation of soil settlement increased.
- The heave of the footing was observed with an increase in matric suction followed by settlement.
- The changing of matric suction due to water conditions with time should be considered while designing of shallow foundations.
- Heave of the foundation was observed when soil conditions changed from saturated to unsaturated.
- ThAe proper drainage system should be provided for the foundation, so that there is a minimum effect of changing water conditions of soil.

Author Contributions: Conceptualization, M.R.H., A.K. and A.F.H.; methodology, M.A. and A.R.G.d.A.; software, R.F., A.S. and M.M.S.S.; validation, M.R.H., M.A. and R.F.; formal analysis, A.K. and Y.A.A.; investigation, Y.A.A. and M.M.S.S.; resources, A.K. and A.R.G.d.A.; data curation, M.M.S.S. and R.F.; writing—original draft preparation, M.R.H. and M.A.; writing—review and editing, M.A., R.F. and M.M.S.S.; visualization, A.K. and A.F.H.; supervision, A.K. and A.S.; project administration, M.A. and A.S.; funding acquisition, M.M.S.S. All authors have read and agreed to the published version of the manuscript.

Funding: The research is partially funded by the Ministry of Science and Higher Education of the Russian Federation under the strategic academic leadership program 'Priority 2030' (Agreement 075-15-2021-1333 dated 30 September 2021).

Institutional Review Board Statement: Not applicable.

Informed Consent Statement: Not applicable.

Data Availability Statement: Data are available on special request from the corresponding authors.

Acknowledgments: The authors would like to thank Mehran University of Engineering & Technology, Jamshoro, Pakistan for providing the lab and research facilities.

Conflicts of Interest: The authors declare no conflict of interest.

References

1. Chen, W.-F.; McCarron, W.O. Bearing capacity of shallow foundations. In *Foundation Engineering Handbook*; Springer: Berlin, Germany, 1991; pp. 144–165.
2. Kim, Y.; Park, H.; Jeong, S.J.S. Settlement behavior of shallow foundations in unsaturated soils under rainfall. *Sustainability* **2017**, *9*, 1417.

3. Johnson, K.; Christensen, M.; Sivakugan, N.; Karunasena, W. Simulating the Response of Shallow Foundations Using Finite Element Modelling. Available online: https://www.mssanz.org.au/MODSIM03/Volume_04/C15/03_Johnson_Simulating.pdf. (accessed on 17 July 2003).
4. Ouabel, H.; Zadjaoui, A.; Bendiouis-Benchouk, A. Numerical Estimation of Settlement under a Shallow Foundation by the Pressuremeter Method. *Civ. Eng. J.* **2020**, *6*, 156–163. [CrossRef]
5. Terzaghi, K. *Theoretical Soil Mechanics*; Wiley: New York, NY, USA, 1943.
6. Michalowski, R. An estimate of the influence of soil weight on bearing capacity using limit analysis. *Soils Found.* **1997**, *37*, 57–64. [CrossRef]
7. Michalowski, R. Upper-bound load estimates on square and rectangular footings. *Geotechnique* **2001**, *51*, 787–798. [CrossRef]
8. Martin, C. Exact Bearing Capacity Calculations Using the Method of Characteristics. Available online: http://citeseerx.ist.psu.edu/viewdoc/summary?doi=10.1.1.521.7612 (accessed on 1 January 2005).
9. Zafeirakos, A.; Gerolymos, N. Bearing strength surface for bridge caisson foundations in frictional soil under combined loading. *Acta Geotech.* **2016**, *11*, 1189–1208. [CrossRef]
10. Zhou, H.; Zheng, G.; Yin, X.; Jia, R.; Yang, X. The bearing capacity and failure mechanism of a vertically loaded strip footing placed on the top of slopes. *Comput. Geotech.* **2018**, *94*, 12–21. [CrossRef]
11. Sultana, P.; Dey, A.K. Estimation of ultimate bearing capacity of footings on soft clay from plate load test data considering variability. *Indian Geotech. J.* **2019**, *49*, 170–183. [CrossRef]
12. Papadopoulou, K.; Gazetas, G. Shape effects on bearing capacity of footings on two-layered clay. *Geotech. Geol. Eng.* **2020**, *38*, 1347–1370. [CrossRef]
13. Fu, D.; Zhang, Y.; Yan, Y. Bearing capacity of a side-rounded suction caisson foundation under general loading in clay. *Comput. Geotech.* **2020**, *123*, 103543. [CrossRef]
14. Li, S.; Yu, J.; Huang, M.; Leung, C. Upper bound analysis of rectangular surface footings on clay with linearly increasing strength. *Comput. Geotech.* **2021**, *129*, 103896. [CrossRef]
15. Das, B.; Sivakugan, N. Settlements of shallow foundations on granular soil—An overview. *Int. J. Geotech. Eng.* **2007**, *1*, 19–29. [CrossRef]
16. Das, B.M. *Principles of Foundation Engineering*; Cengage Learning: Boston, MA, USA, 2015.
17. Mohammed, M.; Sharafati, A.; Al-Ansari, N.; Yaseen, Z.M. Shallow Foundation Settlement Quantification: Application of Hybridized Adaptive Neuro-Fuzzy Inference System Model. *Adv. Civ. Eng.* **2020**, *2020*, 7381617. [CrossRef]
18. Dodagoudar, G.R.; Shyamala, B. Finite element reliability analysis of shallow foundation settlements. *Int. J. Geotech. Eng.* **2015**, *9*, 316–326. [CrossRef]
19. Vanapalli, S.K.; Mohamed, F.M. Bearing capacity of model footings in unsaturated soils. In *Experimental Unsaturated Soil Mechanics*; Springer: Berlin, Germany, 2007; pp. 483–493.
20. Kim, Y.; Jeong, S.; Kim, J. Coupled infiltration model of unsaturated porous media for steady rainfall. *Soils Found.* **2016**, *56*, 1071–1081. [CrossRef]
21. Mahmoudabadi, V.; Ravichandran, N. Design of shallow foundation considering site-specific rainfall and water table data: Theoretical framework and application. *Int. J. Geomech.* **2019**, *19*, 04019063. [CrossRef]
22. Oh, W.T.; Vanapalli, S.K. Modeling the stress versus settlement behavior of shallow foundations in unsaturated cohesive soils extending the modified total stress approach. *Soils Found.* **2018**, *58*, 382–397. [CrossRef]
23. Oh, W.T.; Vanapalli, S.K.; Puppala, A.J. Semi-empirical model for the prediction of modulus of elasticity for unsaturated soils. *Can. Geotech. J.* **2009**, *46*, 903–914. [CrossRef]
24. Schanz, T.; Lins, Y.; Vanapalli, S. Bearing capacity of a strip footing on an unsaturated sand. In *Unsaturated Soils*; Two Volume Set; CRC Press: Boca Raton, FL, USA, 2010; pp. 1195–1200.
25. Schneider-Muntau, B.; Bathaeian, I. Simulation of settlement and bearing capacity of shallow foundations with soft particle code (SPARC) and FE. *GEM-Int. J. Geomath.* **2018**, *9*, 359–375. [CrossRef]
26. Kristić, I.L.; Prskalo, M.; Szavits-Nossan, V. Calibration of Numerical Modeling and a New Direct Method for Calculation of Shallow Foundation Settlements in Sand. 2019. Available online: https://www.issmge.org/uploads/publications/1/45/06-technical-committee-03-tc103-21.pdf (accessed on 24 April 2019).
27. Griffiths, D. Computation of collapse loads in geomechanics by finite elements. *Ingenieur-Archiv* **1989**, *59*, 237–244. [CrossRef]
28. Sloan, S.; Randolph, M.F. Numerical prediction of collapse loads using finite element methods. *Int. J. Numer. Anal. Methods Geomech.* **1982**, *6*, 47–76. [CrossRef]
29. Frydman, S.; Burd, H.J. Numerical studies of bearing-capacity factor N_γ. *J. Geotech. Geoenviron. Eng.* **1997**, *123*, 20–29. [CrossRef]
30. Fok, Y.-S. One-dimensional infiltration into layered soils. *J. Irrig. Drain. Div.* **1970**, *96*, 121–129. [CrossRef]
31. Aylor, D.E.; Parlange, J.Y. Vertical infiltration into a layered soil. *Soil Sci. Soc. Am. J.* **1973**, *37*, 673–676. [CrossRef]
32. Hachum, A.Y.; Alfaro, J.F. Rain infiltration into layered soils: Prediction. *J. Irrig. Drain. Div.* **1980**, *106*, 311–319. [CrossRef]
33. Samani, Z.; Cheraghi, A.; Willardson, L. Water movement in horizontally layered soils. *J. Irrig. Drain. Eng.* **1989**, *115*, 449–456. [CrossRef]
34. Corradini, C.; Melone, F.; Smith, R. Modeling local infiltration for a two-layered soil under complex rainfall patterns. *J. Hydrol.* **2000**, *237*, 58–73. [CrossRef]

35. Ku, C.-Y.; Tsai, Y.-H. Solving nonlinear problems with singular initial conditions using a perturbed scalar homotopy method. *Int. J. Nonlinear Sci. Numer. Simul.* **2013**, *14*, 367–375. [CrossRef]
36. Ghanem, R.G.; Spanos, P.D. *Stochastic Finite Elements: A Spectral Approach*; Courier Corporation: North Chelmsford, MA, USA, 2003.
37. Papadrakakis, M.; Papadopoulos, V. Robust and efficient methods for stochastic finite element analysis using Monte Carlo simulation. *Comput. Methods Appl. Mech. Eng.* **1996**, *134*, 325–340. [CrossRef]
38. Matthies, H.G.; Brenner, C.E.; Bucher, C.G.; Soares, C.G. Uncertainties in probabilistic numerical analysis of structures and solids-stochastic finite elements. *Struct. Saf.* **1997**, *19*, 283–336. [CrossRef]
39. Assimaki, D.; Pecker, A.; Popescu, R.; Prevost, J. Effects of spatial variability of soil properties on surface ground motion. *J. Earthq. Eng.* **2003**, *7*, 1–44. [CrossRef]
40. Simões, J.; Neves, L.C.; Antão, A.N.; Guerra, N.M. Reliability assessment of shallow foundations on undrained soils considering soil spatial variability. *Comput. Geotech.* **2020**, *119*, 103369. [CrossRef]
41. Ali, A.; Lyamin, A.; Huang, J.; Li, J.; Cassidy, M.; Sloan, S. Probabilistic stability assessment using adaptive limit analysis and random fields. *Acta Geotech.* **2017**, *12*, 937–948. [CrossRef]
42. Brantson, E.T.; Ju, B.; Wu, D.; Gyan, P.S. Stochastic porous media modeling and high-resolution schemes for numerical simulation of subsurface immiscible fluid flow transport. *Acta Geophys.* **2018**, *66*, 243–266. [CrossRef]
43. Savvides, A.-A.; Papadrakakis, M. Probabilistic Failure Estimation of an Oblique Loaded Footing Settlement on Cohesive Geomaterials with a Modified Cam Clay Material Yield Function. *Geotechnics* **2021**, *1*, 17. [CrossRef]
44. Savvides, A.-A.; Papadrakakis, M. Uncertainty Quantification of Failure of Shallow Foundation on Clayey Soils with a Modified Cam-Clay Yield Criterion and Stochastic FEM. *Geotechnics* **2022**, *2*, 16. [CrossRef]
45. Sivakugan, N.; Johnson, K. Settlement predictions in granular soils: A probabilistic approach. *Geotechnique* **2004**, *54*, 499–502. [CrossRef]
46. Enkhtur, O.; Nguyen, T.D.; Kim, J.M.; Kim, S.R. Evaluation of the settlement influence factors of shallow foundation by numerical analyses. *KSCE J. Civ. Eng.* **2013**, *17*, 85–95. [CrossRef]
47. Chu, H.-H.; Zhao, T.-H.; Chu, Y.-M. Sharp bounds for the Toader mean of order 3 in terms of arithmetic, quadratic and contraharmonic means. *Math. Slovaca* **2020**, *70*, 1097–1112. [CrossRef]
48. Chu, Y.; Zhao, T. Concavity of the error function with respect to Hölder means. *Math. Inequal. Appl.* **2016**, *19*, 589–595. [CrossRef]
49. Chu, Y.; Zhao, T.; Liu, B. Optimal bounds for Neuman-Sándor mean in terms of the convex combination of logarithmic and quadratic or contra-harmonic means. *J. Math. Inequal.* **2014**, *8*, 201–217. [CrossRef]
50. Chu, Y.-M.; Shankaralingappa, B.; Gireesha, B.; Alzahrani, F.; Khan, M.I.; Khan, S.U. Combined impact of Cattaneo-Christov double diffusion and radiative heat flux on bio-convective flow of Maxwell liquid configured by a stretched nano-material surface. *Appl. Math. Comput.* **2022**, *419*, 126883. [CrossRef]
51. Chu, Y.-M.; Wang, H.; Zhao, T.-H. Sharp bounds for the Neuman mean in terms of the quadratic and second Seiffert means. *J. Inequalities Appl.* **2014**, *2014*, 299. [CrossRef]
52. Chu, Y.-M.; Zhao, T.-H. Convexity and concavity of the complete elliptic integrals with respect to Lehmer mean. *J. Inequalities Appl.* **2015**, *2015*, 396. [CrossRef]
53. Iqbal, M.A.; Wang, Y.; Miah, M.M.; Osman, M.S. Study on Date–Jimbo–Kashiwara–Miwa Equation with Conformable Derivative Dependent on Time Parameter to Find the Exact Dynamic Wave Solutions. *Fractal Fract.* **2022**, *6*, 4. [CrossRef]
54. Nazeer, M.; Hussain, F.; Khan, M.I.; El-Zahar, E.R.; Chu, Y.-M.; Malik, M. Theoretical study of MHD electro-osmotically flow of third-grade fluid in micro channel. *Appl. Math. Comput.* **2022**, *420*, 126868. [CrossRef]
55. Zha, T.-H.; Castillo, O.; Jahanshahi, H.; Yusuf, A.; Alassafi, M.O.; Alsaadi, F.E.; Chu, Y.-M. A fuzzy-based strategy to suppress the novel coronavirus (2019-NCOV) massive outbreak. *Appl. Comput. Math.* **2021**, *20*, 160–176.
56. Zhao, T.; Wang, M.; Chu, Y. On the bounds of the perimeter of an ellipse. *Acta Math. Sci.* **2022**, *42*, 491–501. [CrossRef]
57. Quevedo, R.; Romanel, C.; Roehl, D. Numerical modeling of unsaturated soil behavior considering different constitutive models. In *MATEC Web of Conferences*; EDP Sciences: Les Ulis, France, 2021.
58. Ravichandran, N.; Vickneswaran, T.; Marathe, S.; Jella, V.S. Numerical Analysis of Settlement Response of Shallow Footing Subjected to Heavy Rainfall and Flood Events. *Int. J. Geosci.* **2021**, *12*, 138–158. [CrossRef]
59. Sabri, M.M.; Shashkin, K.G. The Mechanical Properties of the Expandable Polyurethane Resin Based on Its Volumetric Expansion Nature. *Mag. Civ. Eng.* **2020**, *98*, 11. [CrossRef]
60. Sabri, M.M.; Shashkin, K.G. Improvement of the Soil Deformation Modulus Using an Expandable Polyurethane Resin. *Mag. Civ. Eng.* **2018**, *83*, 222–234. [CrossRef]
61. Sabri, M.M.; Shashkin, K.G.; Zakharin, E.; Ulybin, A.V. Soil Stabilization and Foundation Restoration Using an Expandable Polyurethane Resin. *Mag. Civ. Eng.* **2018**, *82*, 68–80. [CrossRef]
62. Sabri, M.M. Subsoil stabilized by polyurethane resin injection: FEM calculations. *Constr. Uniuqe Build. Struct.* **2020**, *91*, 9108. [CrossRef]
63. Ahmad, H.; Asghar, M.U.; Asghar, M.Z.; Khan, A.; Mosavi, A.H. A Hybrid Deep Learning Technique for Personality Trait Classification From Text. *IEEE Access* **2021**, *9*, 146214–146232. [CrossRef]
64. Ahmed, H.U.; Mohammed, A.A.; Rafiq, S.; Mohammed, A.S.; Mosavi, A.; Sor, N.H.; Qaidi, S. Compressive Strength of Sustainable Geopolymer Concrete Composites: A State-of-the-Art Review. *Sustainability* **2021**, *13*, 13502. [CrossRef]

65. Aram, F.; Solgi, E.; Garcia, E.H.; Mosavi, A. Urban heat resilience at the time of global warming: Evaluating the impact of the urban parks on outdoor thermal comfort. *Environ. Sci. Eur.* **2020**, *32*, 117. [CrossRef]
66. Azareh, A.; Sardooi, E.R.; Gholami, H.; Mosavi, A.; Shahdadi, A.; Barkhori, S. Detection and prediction of lake degradation using landscape metrics and remote sensing dataset. *Environ. Sci. Pollut. Res.* **2021**, *28*, 27283–27298. [CrossRef]
67. Darban, S.; Tehrani, H.G.; Karballaeezadeh, N.; Mosavi, A. Application of Analytical Hierarchy Process for Structural Health Monitoring and Prioritizing Concrete Bridges in Iran. *Appl. Sci.* **2021**, *11*, 8060. [CrossRef]
68. Dehghan Manshadi, M.; Ghassemi, M.; Mousavi, S.M.; Mosavi, A.H.; Kovacs, L. Predicting the Parameters of Vortex Bladeless Wind Turbine Using Deep Learning Method of Long Short-Term Memory. *Energies* **2021**, *14*, 4867. [CrossRef]
69. Ghaemi, A.; Zhian, T.; Pirzadeh, B.; Monfared, S.H.; Mosavi, A. Reliability-based design and implementation of crow search algorithm for longitudinal dispersion coefficient estimation in rivers. *Environ. Sci. Pollut. Res.* **2021**, *28*, 35971–35990. [CrossRef]
70. Janizadeh, S.; Pal, S.C.; Saha, A.; Chowdhuri, I.; Ahmadi, K.; Mirzaei, S.; Mosavi, A.H.; Tiefenbacher, J.P. Mapping the spatial and temporal variability of flood hazard affected by climate and land-use changes in the future. *J. Environ. Manag.* **2021**, *298*, 113551. [CrossRef]
71. Kalbasi, R.; Jahangiri, M.; Mosavi, A.; Dehshiri, S.J.H.; Dehshiri, S.S.H.; Ebrahimi, S.; Etezadi, Z.A.-S.; Karimipour, A. Finding the best station in Belgium to use residential-scale solar heating, one-year dynamic simulation with considering all system losses: Economic analysis of using ETSW. *Sustain. Energy Technol. Assess.* **2021**, *45*, 101097. [CrossRef]
72. Khosravi, K.; Golkarian, A.; Booij, M.J.; Barzegar, R.; Sun, W.; Yaseen, Z.M.; Mosavi, A. Improving daily stochastic streamflow prediction: Comparison of novel hybrid data-mining algorithms. *Hydrol. Sci. J.* **2021**, *66*, 1457–1474. [CrossRef]
73. Peng, Y.; Ghahnaviyeh, M.B.; Ahmad, M.N.; Abdollahi, A.; Bagherzadeh, S.A.; Azimy, H.; Mosavi, A.; Karimipour, A. Analysis of the effect of roughness and concentration of Fe_3O_4/water nanofluid on the boiling heat transfer using the artificial neural network: An experimental and numerical study. *Int. J. Therm. Sci.* **2021**, *163*, 106863. [CrossRef]
74. Shahbazpanahi, S.; Tajara, M.K.; Faraj, R.H.; Mosavi, A. Studying the C–H crystals and mechanical properties of sustainable concrete containing recycled coarse aggregate with used nano-silica. *Crystals* **2021**, *11*, 122. [CrossRef]
75. Tavoosi, J.; Suratgar, A.A.; Menhaj, M.B.; Mosavi, A.; Mohammadzadeh, A.; Ranjbar, E. Modeling renewable energy systems by a self-evolving nonlinear consequent part recurrent type-2 fuzzy system for power prediction. *Sustainability* **2021**, *13*, 3301. [CrossRef]
76. Meiabadi, M.S.; Moradi, M.; Karamimoghadam, M.; Ardabili, S.; Bodaghi, M.; Shokri, M.; Mosavi, A.H. Modeling the producibility of 3D printing in polylactic acid using artificial neural networks and fused filament fabrication. *Polymers* **2021**, *13*, 3219. [CrossRef]
77. Mohammadi, M.-R.; Hadavimoghaddam, F.; Pourmahdi, M.; Atashrouz, S.; Munir, M.T.; Hemmati-Sarapardeh, A.; Mosavi, A.H.; Mohaddespour, A. Modeling hydrogen solubility in hydrocarbons using extreme gradient boosting and equations of state. *Sci. Rep.* **2021**, *11*, 17911. [CrossRef]
78. Lu, N.; Likos, W.J. *Unsaturated Soil Mechanics*; John Wiley & Sons, Inc.: Hoboken, NJ, USA, 2004.
79. Briaud, J.-L. *Geotechnical Engineering: Unsaturated and Saturated Soils*; John Wiley & Sons: Hoboken, NJ, USA, 2013.
80. Sivrikaya, O.; Toğrol, E. Determination of Undrained Strength of Fine-Grained Soils by Means of SPT and Its Application in Turkey. *Eng. Geol.* **2006**, *86*, 52–69. [CrossRef]
81. Sivrikaya, O.; Toğrol, E. Relations between SPT-N and qu. In Proceedings of the 5th International Congress on Advances in Civil Engineering, Bangkok, Thailand, 24–25 September 2016.
82. Pusadkar, S.S.; Baral, S.M. Behaviour of Square Footing Resting on Two Layered Clay Deposits. In Proceedings of the 50th Indian Geotechnical Conference, Pune, India, 17–19 December 2015.
83. Janda, T. Modeling of Deep Foundations Founded in Collapsible Soils. Available online: http://citeseerx.ist.psu.edu/viewdoc/download?doi=10.1.1.530.3926&rep=rep1&type=pdf (accessed on 6 February 2008).
84. Loukidis, D.; Lazarou, G.; Bardanis, M. Numerical Simulation of Swelling Soil–Mat Foundation Interaction. Available online: https://www.ecsmge-2019.com/uploads/2/1/7/9/21790806/0461-ecsmge-2019_loukidis.pdf. (accessed on 17 September 2019).
85. Altaweel, A.A.; Shakir, R.R. The Effect of Interference of Shallow Foundation on Settlement of Clay Soil. In *IOP Conference Series: Materials Science and Engineering*; IOP Publishing: Bristol, UK, 2021.
86. Liu, C.-Y.; Ku, C.-Y.; Xiao, J.-E.; Huang, C.-C.; Hsu, S.-M. Numerical modeling of unsaturated layered soil for rainfall-induced shallow landslides. *J. Environ. Eng. Landsc. Manag.* **2017**, *25*, 329–341. [CrossRef]
87. Mahmoudabadi, V.; Ravichandran, N. Coupled Geotechnical-Hydrological Design of Shallow Foundation Considering Site Specific Data—Theoretical Framework and Application. *J. GeoEng.* **2018**, *13*, 93–103.
88. Mehndiratta, S.; Sawant, V.A. Numerical modelling of mechanical behaviour of partially saturated soils using coupled FEA. *Int. J. Geotech. Eng.* **2017**, *11*, 452–466. [CrossRef]